Verification and Validation of CFD Software by ONERA, DLR, Airbus for Helicopter Fuselages

Lukas Rottmann
Institute of Aerodynamics and Flow Technology
German Aerospace Center (DLR) Braunschweig
Lilienthalplatz 7, 38108 Braunschweig, Germany
lukas.rottmann@dlr.de

Abstract

An extended stencil in Green-Gauss reconstruction and the matrix-free GMRES block Jacobi method are recent advances in CFD, which have been implemented into the new **C**FD software by **O**NERA, **D**LR and **A**irbus (CODA). The GOAHEAD helicopter fuselage configuration, which was measured in the wind tunnel, is computed with CODA and compared against results generated with DLR's legacy flow solvers FLOWer and TAU.

1. INTRODUCTION

The design of efficient helicopters to reduce emissions continues to be a major challenge for the aerospace industry. Previous studies on light twin-engine helicopters have shown that the fuselage and rotor head as well as the landing skids play an important role in the drag of a helicopter [1]. The reduction of parasitic drag of the individual components as well as their interaction has become a focal point for helicopter research in recent years in order to minimize the impact of rotorcraft traffic on the environment. In order to understand this parasitic drag, numerous wind tunnel tests and computational fluid dynamics (CFD) simulations have been carried out in the past. The wind tunnel tests were used to validate the CFD methods and algorithms, but also to gain insight into the flow physics themselves. The steady-state simulations of the RANS equations using different turbulence models for isolated fuselages have become an established tool for the drag prediction of helicopter fuselages. However, less established methods such as DDES simulations are also used and are compared with RANS and URANS simulations by Fuchs et al. [2]. In addition to comparing different turbulence models, the comparison between CFD solvers is also important to compare the implementation of the methods. In the overview of different fuselages and simulations in the publication by Batrakov et al [3], some configurations were also simulated with different CFD solvers. Due to different solver architectures or configurations, comparisons were sometimes performed on different or similar CFD meshes. In addition, mesh convergence was not examined in any cases [4]. From DLR's experience over the last two decades in the simulation of helicopter fuselages [5] [6] [7] [8], no satisfactory convergence of the residuals of the conservative flow variables could be achieved, especially when solving RANS-based CFD simulations. ONERA, DLR, and Airbus are developing a new common CFD code CODA [9] [10] that besides improved accuracy by using an extended stencil in the Green-Gauss reconstruction [11], features a stronger solution methodology. In this work, the capabilities of this new code are demonstrated for the GOAHEAD [12] fuselage configuration that has been measured in the wind tunnel, but also with results produced by the DLR legacy flow solvers FLOWer [13] and TAU [14]. Furthermore, a mesh convergence study is carried out for TAU and CODA, using the same meshes for both solvers. Subsequently, polar simulations for TAU and CODA are also compared with the experiment on the same meshes

2. CODA

CODA is part of a new generation of flow solvers that combines the cell-centered metric method for established finite volume (FV) schemes with high-order discontinuous Galerkin (DG) methods on unstructured meshes. Special emphasis is placed on efficient simulations on heterogeneous HPC structures in a highly parallelized environment. For the discretization of convective fluxes, multiple schemes are available. In this paper the finite volume formulation of Roe's (upwinding) scheme is employed. For the gradient-based reconstruction of the state values at the left and right cell surface, the extended Green-Gauss gradient method is used. The "spline quantic" limiter is applied to limit the gradients. The temporal integration is performed using an linearized implicit Euler scheme based on the matrix-free GMRES block Jacobi method. The selected parameter setup is mainly based on the investigations of Volpiani Pedro [9] [10]. All flow simulations performed are fully turbulent. The Spalart-Allmaras (SA) one equation turbulence is used in the negative formulation [15] for both the novel CODA and TAU results. All CODA results shown are converged by at least eleven orders of magnitude in the residuals of the conservative flow variables. The results of the turbulence equation are also reduced to these orders of magnitude.

3. GOAHEAD

GOAHEAD stands for **G**eneration **o**f an **a**dvanced **h**elicopter **e**xperimental **a**erodynamic **d**ata base for CFD validation. This European project aimed to improve the aerodynamic predictability of the European helicopter industry with regard to complete helicopter configurations. This project provides a good basis [12] for the validation of 3D CFD simulations with its extensive database. Thus, the validation with CODA joins a series of validations with the established legacy codes. The isolated fuselage was examined with FLOWer and TAU in the blind test phase. In the past, three Mach numbers were simulated, each with a different angle of attack [16] [17]. On the other hand, the influence of the rotor on the fuselage was investigated [18]. In this paper, the entire polar curve of the TC1 test case is validated. The TC1 test case includes an isolated fuselage in forward flight at a Mach number of $Ma = 0.204$ at different angles of attack between $\alpha_f = -10.9°$ und $\alpha_f = 8.8°$.

4. INVESTIGATION

The aim is to re-evaluate the GOAHEAD fuselage configuration with CODA and TAU with respect to the past investigations with TAU and FLOWER, thus to validate CODA as a new CFD solver and identify the benefits of the new methods available. For this purpose, a mesh sequence of unstructured meshes are created with "Pointwise" that could be used for both CFD codes, CODA (cell-centered) and TAU (cell-vertex). The mesh sequence contains three meshes with different numbers of mesh points and mesh elements. Since the results of the wind tunnel experiments were not corrected afterwards, it is important to simulate the wind tunnel walls in the CFD simulation in order to be able to compare the results with the experiments. While for structured grids a mesh sequence can easily be generated by skipping every other grid point in each index direction from the finest mesh, and repeating this for consecutive refinement levels, this is not automatically given for unstructured grids. In order to ensure consistence of the various grids when employing the unstructured grid approach, the grid has been split into three different areas for refinement. Figure *1* shows the three different areas. The wind tunnel is divided into: a part in front of the fuselage, a part with the fuselage, and a part behind the fuselage.

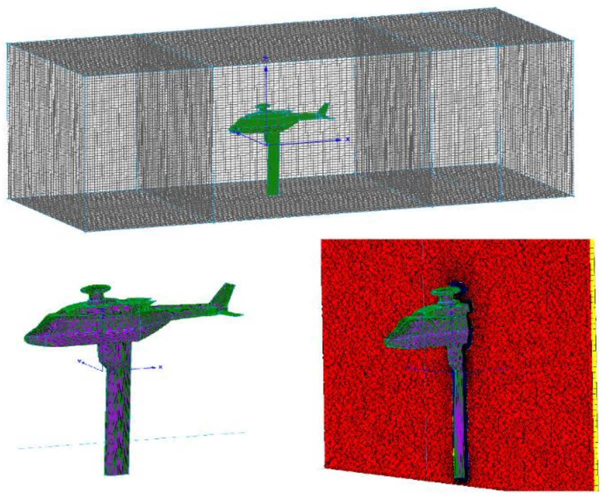

Figure 1: Mesh parts

The fuselage surface is largely discretized with quadrilaterals and in a few areas a combination of triangles and quadrilaterals is used to simplify the meshing. The volume mesh starting from the surface is divided into a solid boundary layer block extruded from the surface and the remaining volume mesh. The boundary layer block has been extended with the anisotropic tetrahedral extrusion (T-Rex) [19] functionality in the field. This simple division makes it possible to approximately increase the number of mesh points between the individual mesh levels by a factor of eight, similar to the structured grid approach. The increase in the number of mesh points was initially carried out using a glyph-script and Pointwise in batch mode, starting from the coarse mesh. Each individual mesh refinement then had to be adjusted manually. The respective numbers of the different mesh levels created this way are shown in Table 1. Comparable mesh convergence studies for isolated fuselage simulations have shown that the convergence of the force coefficients depends significantly on the number of mesh points on the fuselage surface. The level 1 mesh in this study has a factor of three more surface mesh points than the finest mesh from the publication by Renaud et al. [4].

Table 1 Mesh levels

Level	3	2	1
Mesh points	3.5MM	24.6MM	191MM
Elements	7.5MM	52.5MM	394.5MM
Surface points	38K	150.5K	606.6K
Surface elements	104.8K	416.8K	1.7MM

This mesh setup can quickly be regenerated for different angles of attack. In order to achieve this, the boundary layer block was rotated and only the intermediate area between the boundary layer and the wind tunnel walls is remeshed. Twelve angles of attack from minus ten to plus eight degrees were generated and simulated for the Level 3 and Level 2 mesh

5. RESULTS

5.1. MESH CONVERGENCE STUDY

In the following results section, the mesh convergence study for the GOAHEAD fuselage for the approach angle of 0° is analyzed in detail. Figure *2* the results are displayed. The forces were evaluated in the wind tunnel coordinate system and thus represent the lift (C_z), drag (C_x) and lateral force (C_y) coefficient. The moment reference point is located at the origin of the balance of the wind tunnel model. The balance was mounted between the strut and the fuselage in the wind tunnel experiment. This means that only the fuselage is used when considering the individual coefficients and the strut and rotor head is not considered. The rotor head was measured with a separate scale independent of the fuselage scale. The coefficients are plotted against the grid spacing. By using a cell-centered metric in CODA, the grid spacing is formed by the number of grid elements. TAU uses a cell-vertex metric so the grid spacing is formed with the number of grid points. This allows CODA and TAU to be analyzed with their number of unknowns. All coefficients except for lift force (C_z) and lift pitching moment coefficient (cm_y) converge towards the wind tunnel result as the mesh becomes finer. With regard to the force coefficients, there is an almost linear change in the coefficients for CODA, which indicates a convergence of the grid. Whereas TAU does not show this linear convergence on this grid sequence. For the moment coefficients, neither TAU nor CODA show a mesh convergent behavior. For drag and lateral force, the difference between TAU and CODA is minimal on the finest level. The lift force (C_z) exhibits the largest differences between the solvers even on the finest mesh. The difference is due to a different lift coefficient distribution on the fuselage surface. This is caused by the differently resolved vortical flow around the rotor head. Figure *3* shows the comparison of the individual surface parts. The complete configuration includes fuselage, strut and rotor head. It can be seen that the largest difference in the drag coefficient is due to the rotor head, which was not considered in the Figure *2* This also makes the biggest difference in terms of the total configuration on the finest mesh. The fuselage and rotor head have their greatest difference in the lift coefficient. The strut shows only small differences for both coefficients.

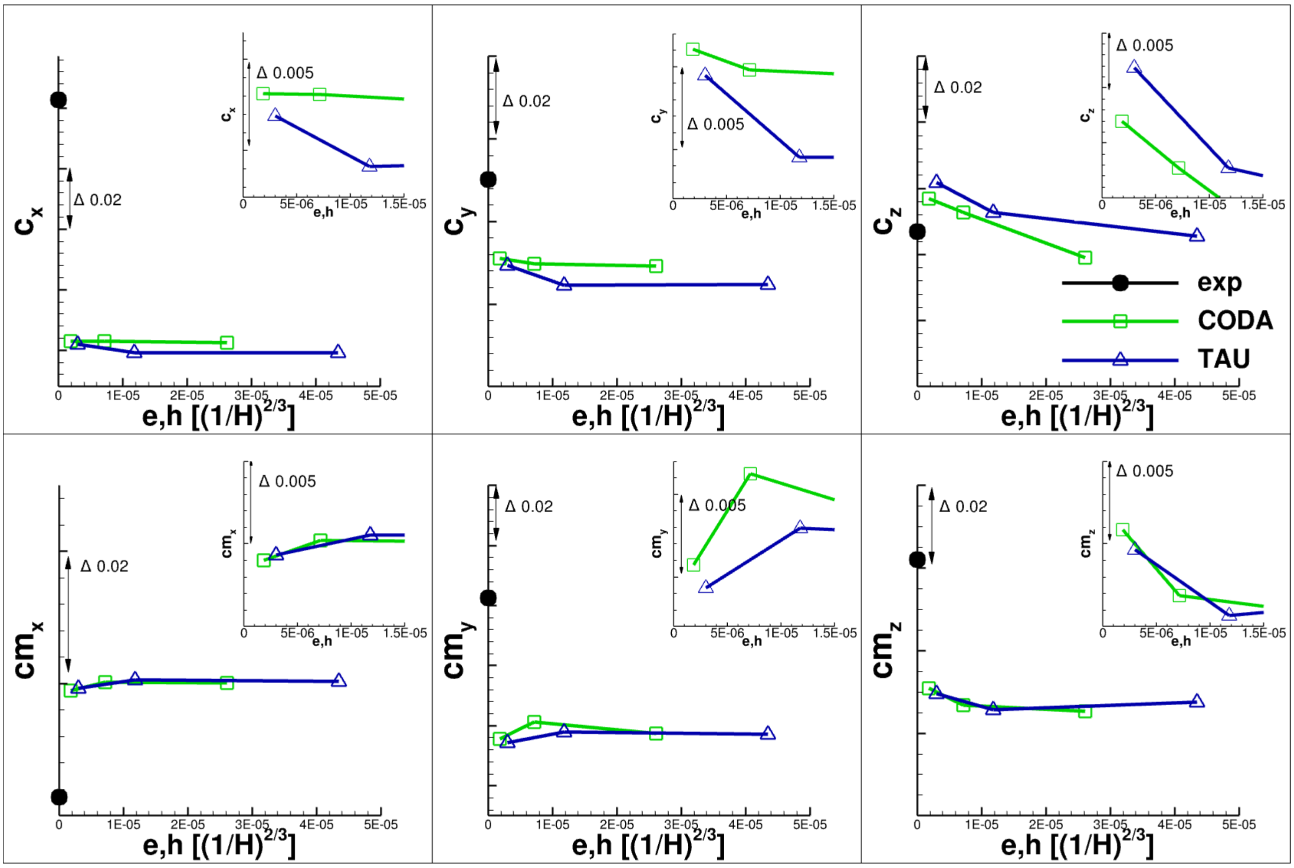

Figure 2: Mesh convergence for force and moment coefficients for the approach angle of 0°

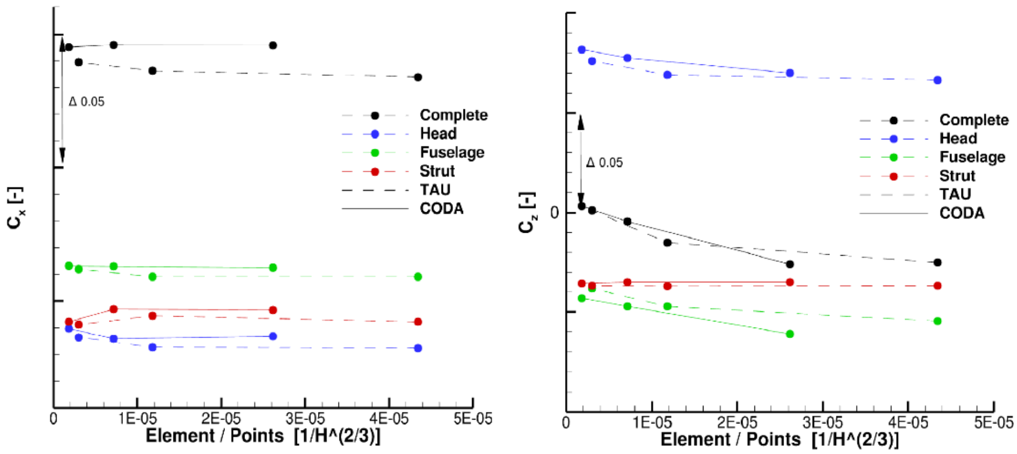

Figure 3: Comparison of the individual fuselage surface parts

Figure *4* shows the vortex trajectories represented by the Q criterion at the same threshold for both solvers. It can be seen that CODA more accurately resolves the vortices on coarser meshes. This is not only evident at first glance for the vortices behind the strut, but also on closer inspection behind the rotor head. This is caused by the different metrics between cell-centered metric for CODA and cell-vertex metric for TAU. Due to the chosen mesh configuration and the largely quadrilateral discretized surface, the boundary layer block contains predominantly hexahedra. The difference between the number of elements and mesh points should therefore be roughly the same in this area. Outside the boundary layer block up to the wind tunnel walls there are predominantly tetrahedra. The tetrahedral section therefore yields more elements for CODA then for TAU, for which it is closely related to the number of grid points. As can be seen in Table 1, the difference between the number of grid points and the number of elements over the entire mesh is about a factor of two. CODA should therefore be able to resolve the flow more precisely in this area due to the higher number of degrees of freedom. A closer look also shows that there are differences in the wake of the rotor head even on the finest mesh between TAU and CODA. These have their origin in a different prediction of the flow separation at the rotor head. And the vortices on the strut are also the result of a flow separation. Figure *5* shows the friction coefficient for TAU and CODA across all mesh levels. Dark blue areas show a negative coefficient of friction and indicate flow separation. The colors from blue to red show an increase in the coefficient of friction and visualize the attached flow. This shows that CODA already calculates separation on coarser meshes in the area of the strut, which is only recognizable in TAU on the finest mesh. It can also be seen that the separation areas at the rotor head differ between TAU and CODA on the finest mesh. Due to this different separation, there are also different wake areas behind the rotor head. This has a great influence on the drag of the rotor head as shown in Figure *3* and is also the reason for the different lift coefficients. The wake area behind the rotor head has a significant influence on the drag of the rotor head and the wake area behind the rotor head has an influence on the pressure distribution of the tail of the fuselage and thus on the lift of the fuselage due to its loss of momentum compared to the undisturbed flow.

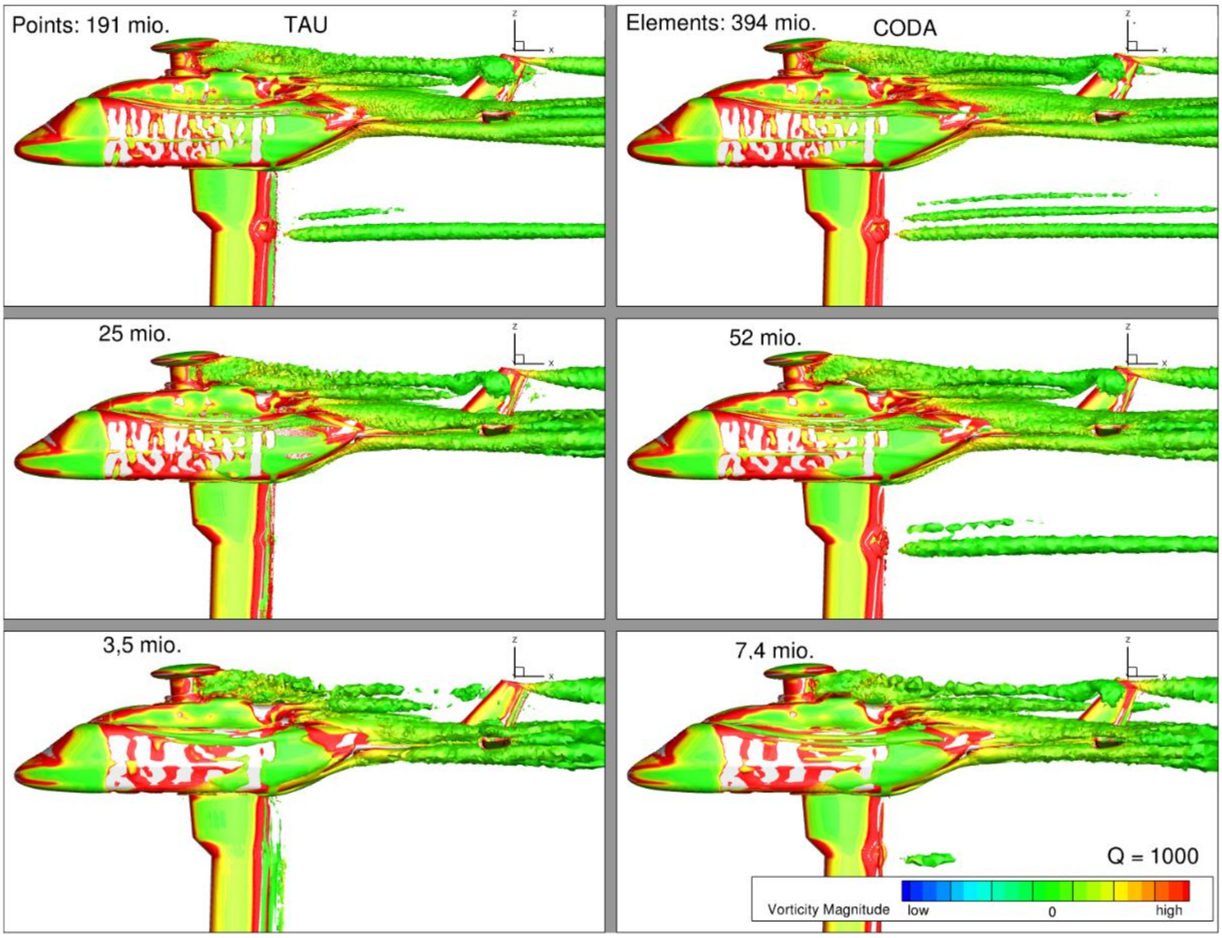

Figure 4: Vortex visualization with the Q criterion

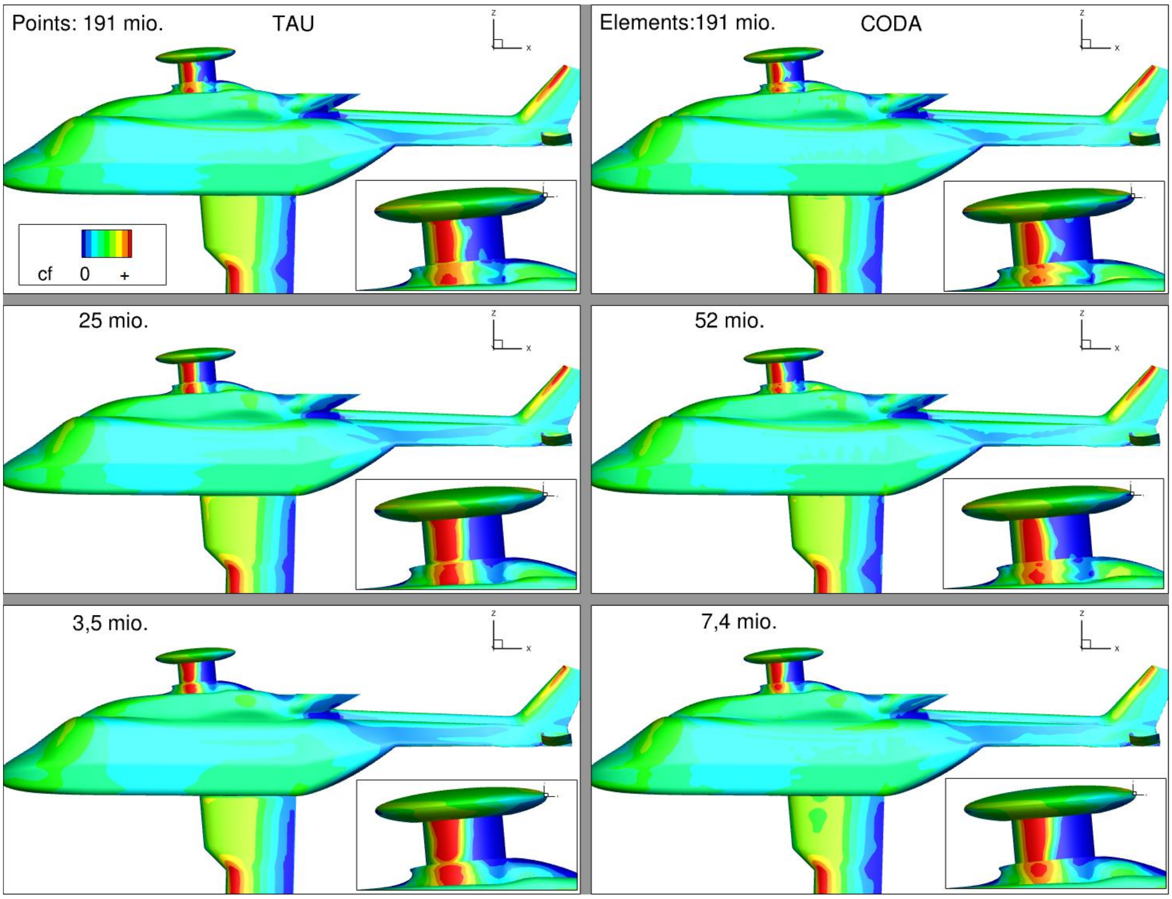

Figure 5: Friction coefficient for TAU and CODA across all mesh levels.

A comparison of the pressure coefficient on the fuselage surface for TAU and CODA also confirms the influence of the rotor head wake on the lift coefficient of the fuselage. Figure *6* shows the location of the pressure measurement holes in the experiment. In Figure *7* displays the result of the pressure measurement sections shown in Figure *6* for TAU across the three mesh levels. The “S2” section and also the “V1” section up to just before the rotor head show slight differences between the individual mesh levels. In section “S4”, “S6” and “S7”, as well as in section “V1” behind the rotor head, there is a clear influence of the different mesh levels. The wake directly behind the rotor head in section “S4” shows only small differences for TAU between level 2 and level 1 and would indicate a grid-convergent behavior. However, this behavior probably only applies to this section. In section V1, there are still clear changes between the mesh levels behind the rotor head. The influence of the wake of the rotor head and the engine outlets on the tail boom is shown in sections “S6” to “S7”. Here, too, there are still clear deviations between the individual mesh levels. In addition, an increasing asymmetry of the pressure distribution can be seen in this area due to the asymmetric configuration in the area of the tail surface.

Compared to TAU, CODA shows significant changes between the mesh levels, especially in the area behind the rotor head as shown in Figure *8* Compared to TAU, CODA appears to be closer to the level 1 results in the wake behind the rotor head with the level 2 results. It is seen that TAU lags behind the CODA results on the level 2 grid, particularly in the wake area. This leads to the assumption that both TAU and CODA are not yet mesh convergent in the area behind the rotor head, whereby CODA is able to resolve the wake better on coarser meshes due to its higher number of degrees of freedom. The not yet grid-converged area behind the rotor head also explains the differences between TAU and CODA on the finest grid, as the difference should be reduced by the higher accuracy due to the Green-Gauss gradient method and the influence of the cell metric at grid convergence. It should also be mentioned here that although CODA converged to eleven orders of magnitude in the residuals, the TAU results were not simulated further from eight orders of magnitude. Tests with the level 3 mesh also showed convergences for TAU in the range of eleven orders of magnitude in the residuals without significant changes in the coefficients between eight and eleven orders of magnitude. Even if the results here lead to the conclusion of a non-mesh-convergent area behind the rotor head, it is questionable whether a next finer level can also be converged to a steady state. It would be possible to refine a mesh only in the area of the rotor head, but this would change the mesh topology and make a comparison more difficult.

In the end, the actual separation is unsteady and forcing a steady solution might be questionable at some point. Deviations from the experiments can be explained by the fact that the position of the fuselage is not exactly the same as in the wind tunnel. In the experiment, the rotor blades were removed for the isolated fuselage tests, but the blade holders were left in place. In these simulations, this area has been simplified using a cylindrical body and also the tail rotor drive has also been disregarded. This leads to the wake of the rotor head is not reproduced exactly in comparison to the experiment

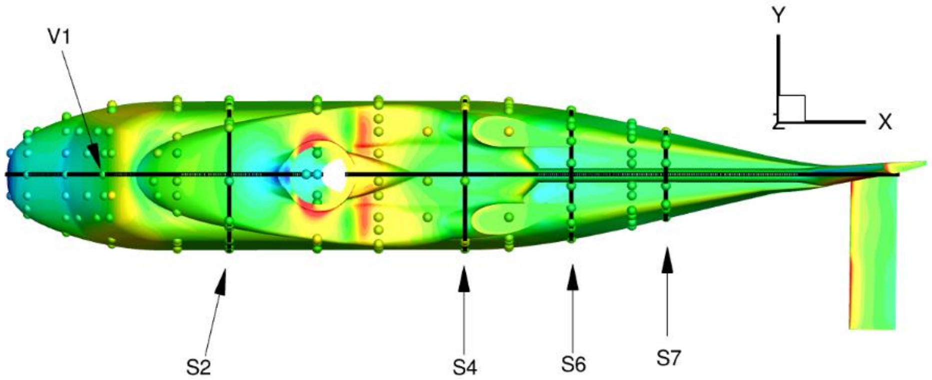

Figure 6: Pressure measurement location

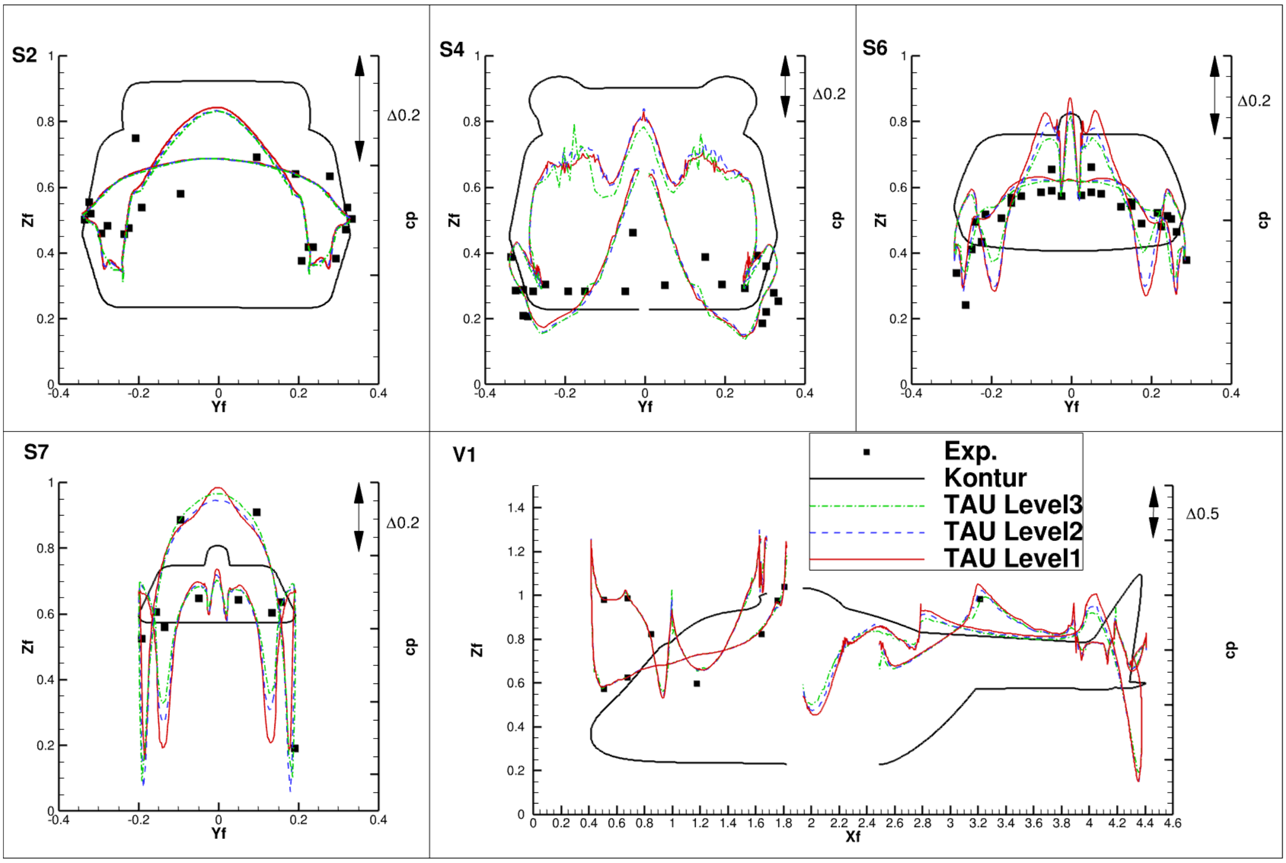

Figure 7: TAU surface pressure coefficient over three mesh levels

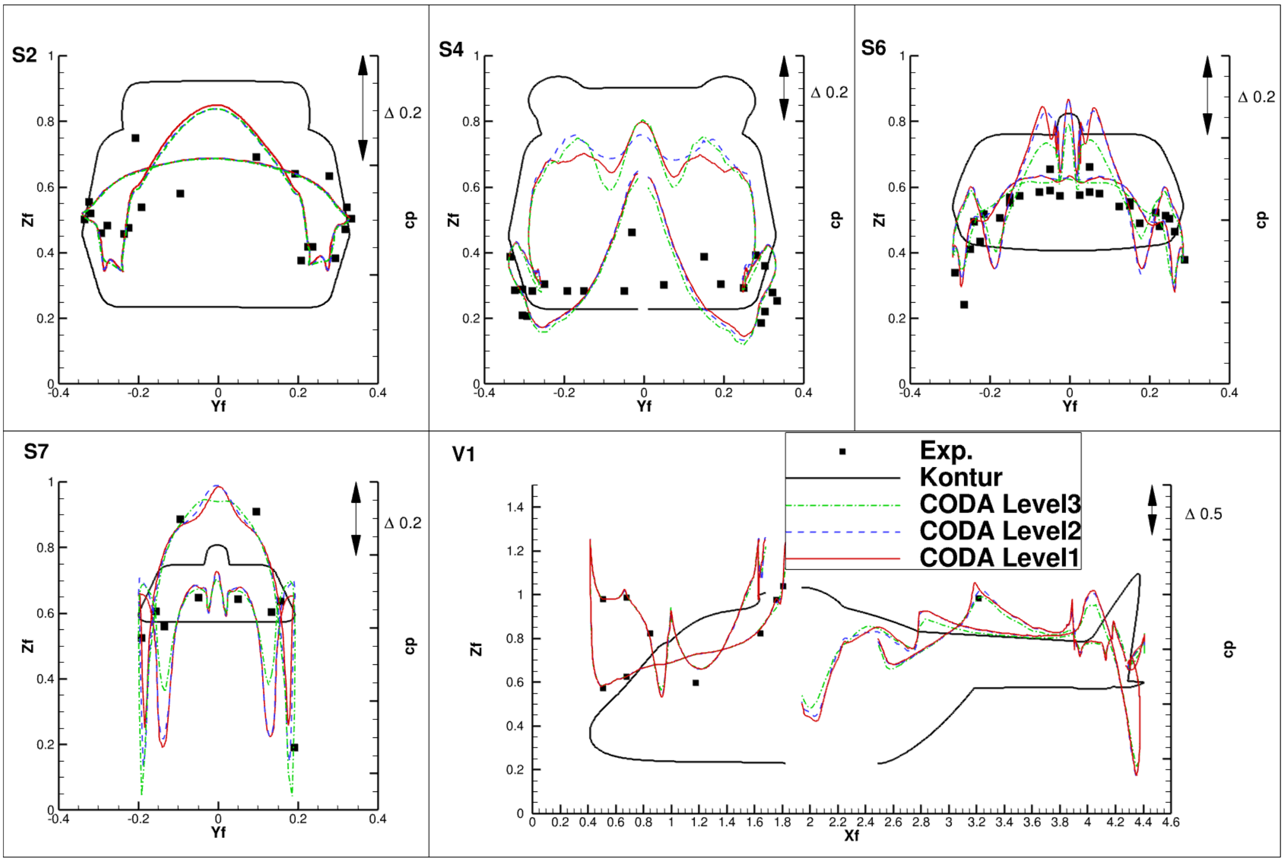

Figure 8: CODA surface pressure coefficient over three mesh levels

5.2. POLAR SIMULATION

In the past, several comparisons were made between TAU and FLOWER with the GOAHEAD configuration. Figure *9* compares the results of TAU and CODA on level 3 mesh with past TAU and FLOWer results, as well as the wind tunnel experiment. The previous results differ from the current simulations in terms of mesh and turbulence model. Overall, the CODA results presented are well within the scatter of the other CFD simulations. It is assumed that the physics within the RANS approach are modelled correctly. Only the Level 3 mesh was compared here, as the number of elements in this mesh is comparable to the number of mesh points in the previous results. Deviations from the experiment can be explained in the same way as in the mesh convergence study. The wind tunnel experiments are used to evaluate the simulation results. An exact reproduction of the experiments is therefore not expected. The influence of the different turbulence modeling is particularly evident in the drag, which shows the greatest deviations from the scattering, especially for larger negative angles of attack.

In addition to the polar simulation on the level 3 mesh, polar simulations were also carried out with the level 2 mesh for TAU and CODA. Figure *10* shows that for TAU between the Level 3 and Level 2 grids there is essentially only a small change in the coefficients across the polar curve. Larger deviations occur at a large angle of attack of around 8 degrees. The influence on the mesh convergence is smallest for the drag coefficient (C_x) while larger changes can be observed for the yaw moment (cm_z). It can be seen that the selected mesh topology for TAU does not show any major deviations even over a larger angle of attack range with the selected mesh refinement. This suggests that the mesh refinement provides the required mesh fineness even at different angles of attack. Only for the eight-degree case does the necessary mesh refinement appear to be insufficient.

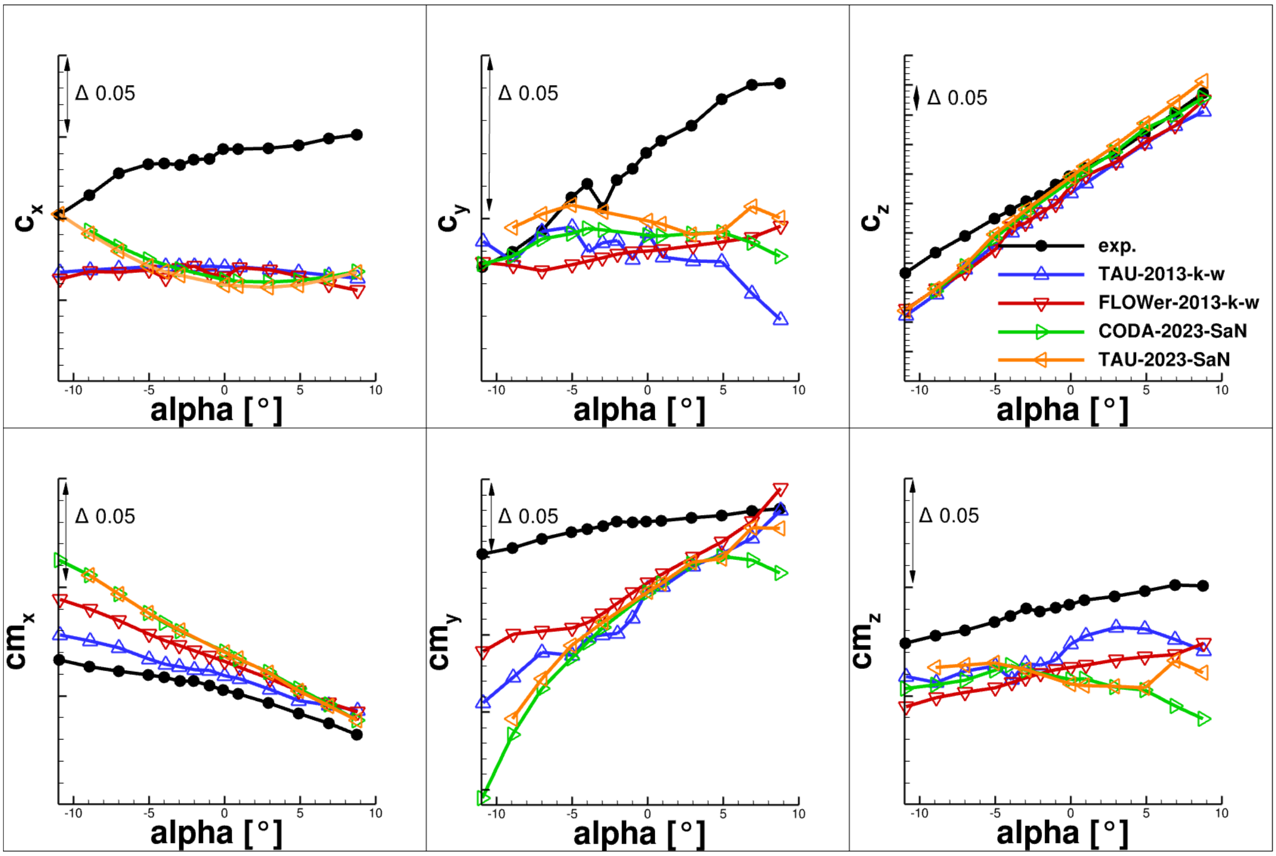

Figure 9: Comparison between TAU, FLOWER and CODA

The greatest differences to the level 1 mesh can be recognized for the lateral force (C_y). It is also noticeable that the differences between the three meshes for an angle of attack of zero degrees are small in relation to the changes in the coefficients over different angles of attack. CODA shows a similar behavior compared to TAU in Figure *11* In contrast to TAU, there are no major deviations at a high angle of attack of 8°. The selected mesh topology does not show any major deviations for CODA over a larger angle of attack range with the selected mesh refinement. For the lateral force, CODA shows greater deviations between the mesh levels in the range from zero degrees to around minus eight degrees. In general, most of the lateral force is generated by the vertical stabilizer. An additional contribution to the lateral force is made by the tail boom, which increasingly shows an asymmetrical pressure distribution in the direction of the tail stabilizer. This asymmetry can be seen most clearly in the mesh convergence study in Figure *7* and Figure *8* in section "S7". This asymmetry is particularly evident in the range between zero degrees and about minus eight degrees. Figure *12* shows the pressure slices through the tail section for slices "S4", "S6" and "S7" for TAU and CODA for an angle of attack of minus five degrees. The major differences between Level 3 and Level 2 meshes in CODA are also evident here in section "S7". It is reasonable to assume that CODA resolves the wake of the rotor head better on coarser meshes and that TAU is behind CODA on the Level 2 mesh as seen in the previously presented mesh convergence study. The biggest differences compared to the Level 1 mesh can be recognized mainly in the yaw moment (cm_z). However, the yaw moment is significantly smaller than the roll moment (cm_x) and pitching moment (cm_y) due to the different angles of attack

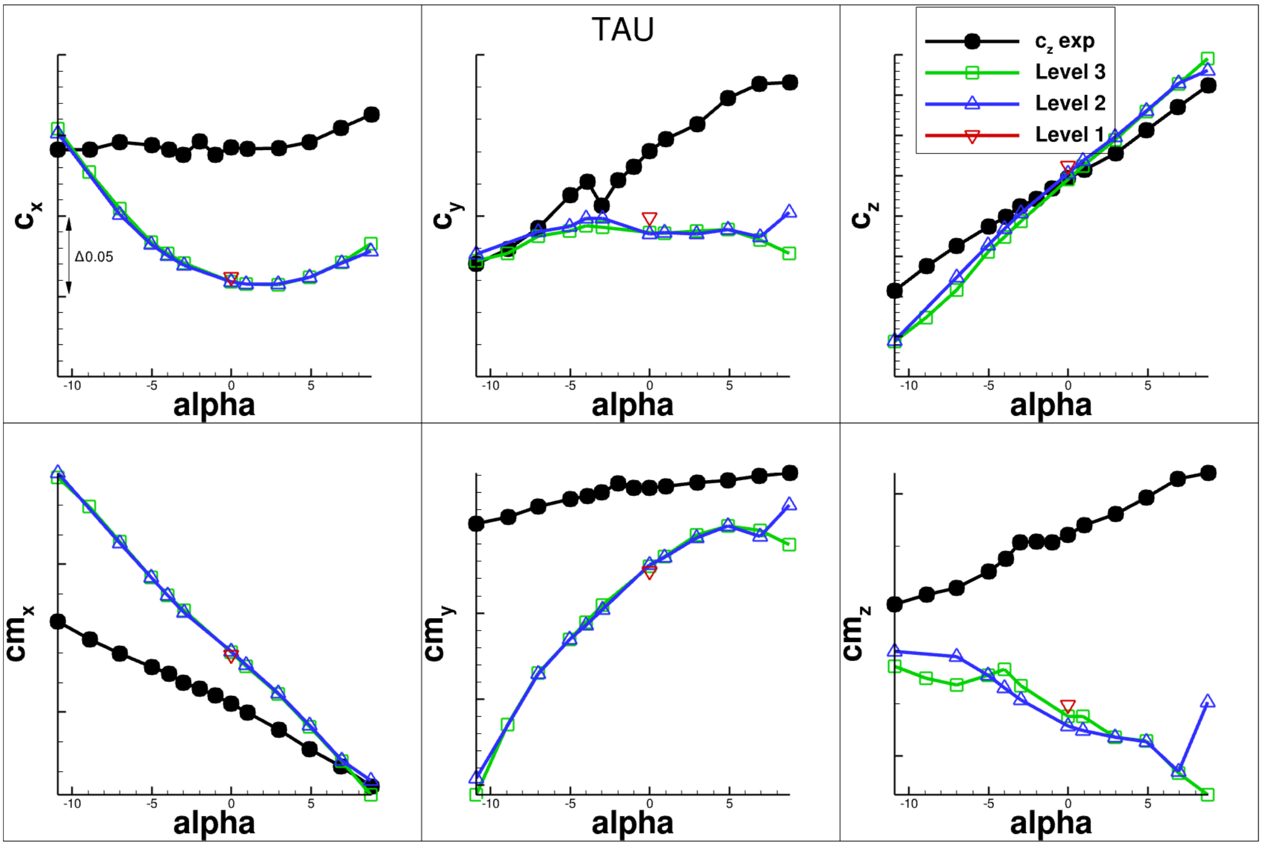

Figure 10: Polar simulation for TAU over three mesh levels

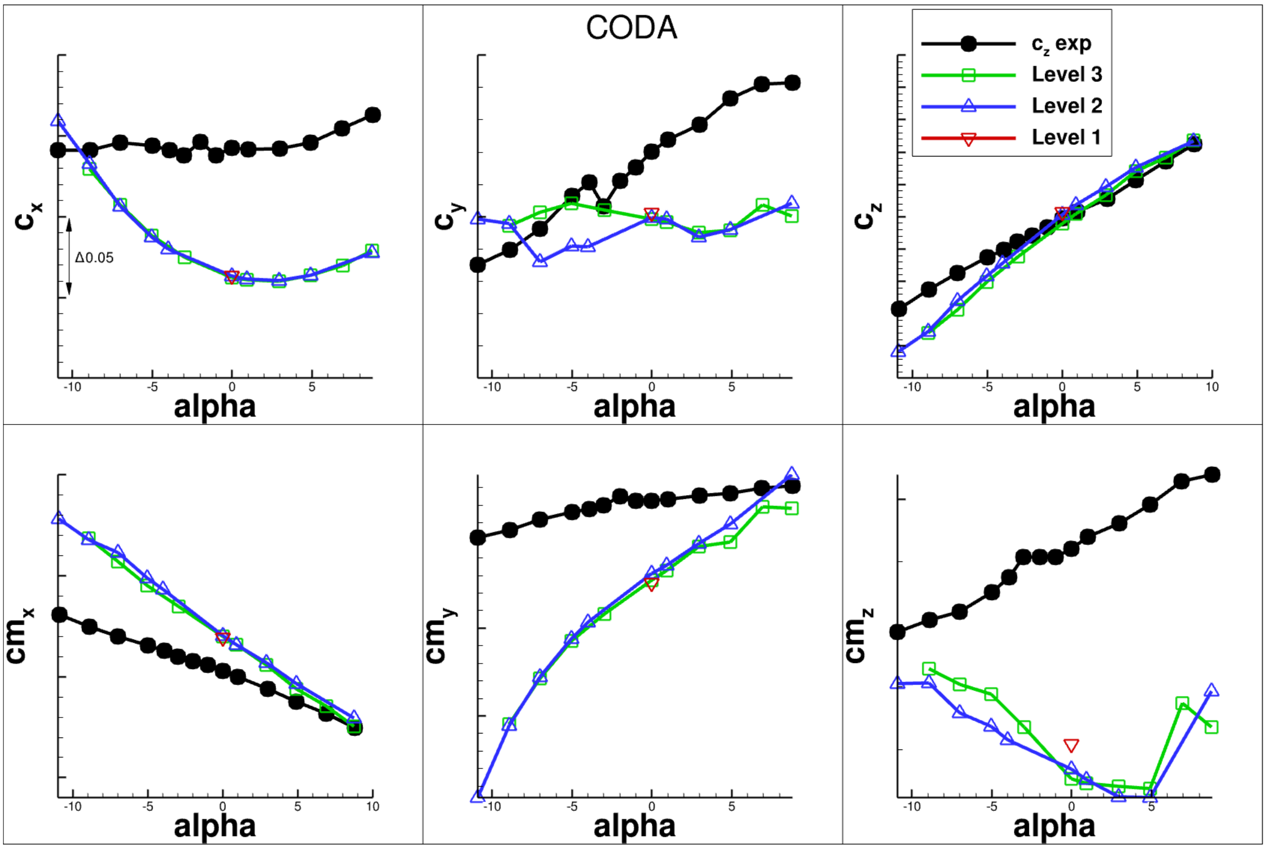

Figure 11: Polar simulation for CODA over three mesh levels

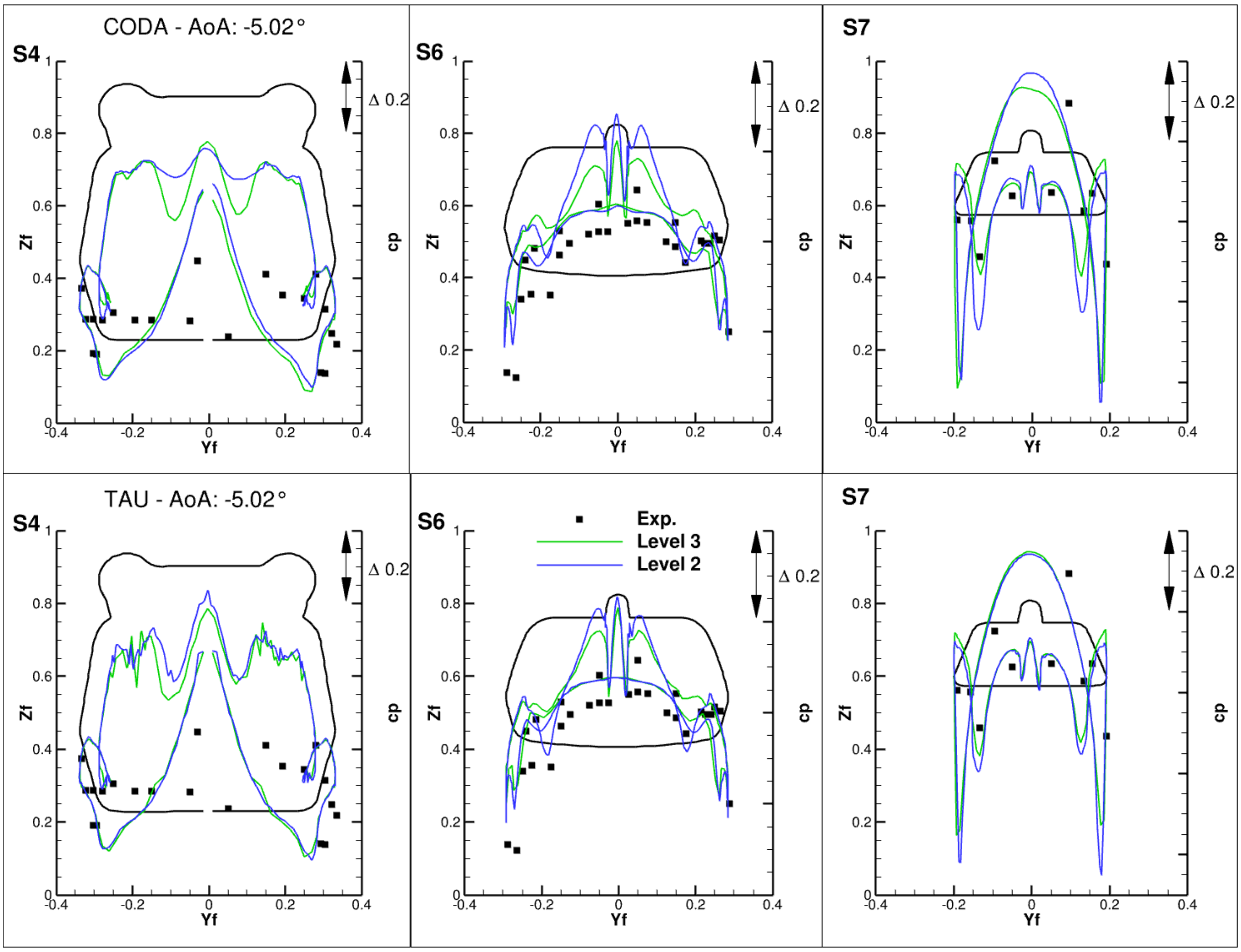

Figure 12: CODA and TAU for level 3 and level 2 the pressure coefficient on the surface for AoA: $-\mathbf{5.02}°$

5.3. SOLVER SCALING

One of the biggest advantages of CODA compared to TAU is that CODA has been optimized for high parallelization and utilizes a hybrid technique of domain decomposition and shared memory application. To accomplish this, simulations were carried out for this GOAHEAD configuration to investigate the scaling of parallel efficiency. For this purpose, the number of computing nodes was increased step by step and the required simulation time was evaluated. These simulations were carried out on the level 3 mesh for TAU and CODA. The simulation duration was determined after a convergence of eleven orders of magnitude in the density residual was achieved for both solvers. Acceleration methods such as multigrid were not used as it is expected that the behavior with respect to processor scaling produces the best results for singlegrid.

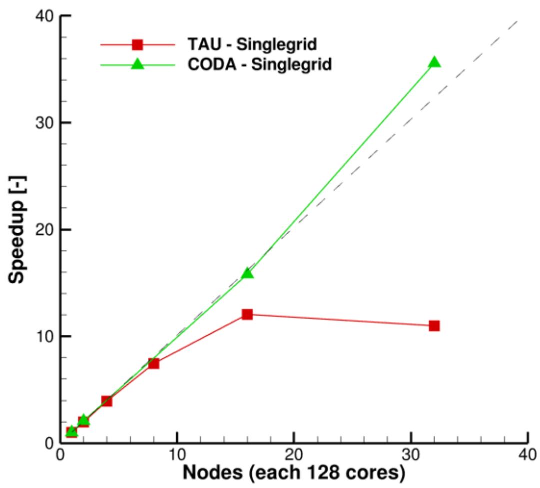

Figure 13: Speedup depending on the computing nodes employed

Figure 13 shows the described behavior. The speedup is plotted over the number of nodes. Each computing node has a number of 2x64 AMD EPYC 7702 (Rome) processors at 2 Ghz. The speedup results from the reciprocal value of the nominated wallclock time. CODA shows a speedup in the linear range even in the area with a very high number of processors or conversely very low number of grid points per core. Around one thousand mesh points remain per core. Whereas TAU no longer shows a speedup, but even a slowdown of the simulation due to communication overheard.

6. SUMMARY

This paper presents for the first time the results of a detailed study of grid convergence at three grid levels and polar simulations using the novel extended Green-Gauss stencil available in the CODA solver compared to wind tunnel experiments for the GOAHEAD configuration. The results are additionally compared to results produced with the legacy flow solver TAU on the same grids. The polar simulations were performed for grid level 3 and level 2 for CODA and TAU. The wind tunnel tests provide data for comparison of scale values and pressure measurements. The main result of this paper is that CODA as a new generation flow solver provides more accurate results for this case and shows a better parallelization than TAU. It was also shown that the chosen mesh topology and refinement remains valid over a wide range of angles of attack. However, it also shows how difficult mesh refinement studies are for unstructured meshes and that the very high number of points on the level 1 mesh in the rotor head area does not yet allow mesh convergence in the strict sense. On a practical level, this studies also reveals that grid points may be more focused behind the rotor head, but in other areas are already sufficiently resolved, therefore allowing for an intermediate grid that has less grid points but the same or better result quality as found on the finest mesh. In terms of scaling with the number of computing nodes, CODA shows its capabilities compared to TAU even with a very high number of processors, allowing a speed-up of the simulation.

Next steps could be to evaluate the capabilities of the DG solution in CODA for the GOAHEAD configuration. Due to the higher order of the solution, it should be possible to resolve the separation behind the rotor head even better on coarse meshes.

7. AKNOWLEDGEMENTS

CODA is the computational fluid dynamics (CFD) software being developed as part of a collaboration between the French Aerospace Lab ONERA, the German Aerospace Center (DLR), Airbus, and their European research partners. CODA is jointly owned by ONERA, DLR and Airbus.

The author would also like to thank Axel Schwöppe for his enduring support with the new solver CODA.

8. REFERENCES

[1] Grawunder M., Reß R., Breitsamter C., Adams N., "Flow Characteristics of a Helicopter Fuselage Configuration Including a Rotating Rotor Head," in 28th Congress of the International Council of the Aeronautical Sciences, Brisbane, Australia, 23 - 28 September 2012.

[2] Fuchs, M., Le Chuiton, F., Mockett, C., Sesterhenn, J., Thiele, F., "Detached-Eddy Simulation of Separated Wake Flow Around Complex Helicopter Fuselage Configuration," in Progress in Hybrid RANS-LES Modelling, Notes on Numerical Fluid Mechanics and Multidisciplinary Design, Vol. 130, p. 131-140, Springer, Berlin/Heidelberg, 2015.

[3] Batrakov, A., Garipova L., Kusyumov A., Mikhailov S., Barakos G., "Computational Fluid Dynamics Modeling of Helicopter Fuselage Drag," in Journal of Aircraft, 2015.

[4] Renaud T., O'Brien D., Smith M., Potsdam M., "Evaluation of Isolated Fuselage and Rotor-Fuselage Interaction Using CFD," in Annual Forum Proceedings - American Helicopter Society, 2004.

[5] Gleize, V. und Costes, M. und von Geyr, H. und Kroll, N. und Renzoni, P. und Amato, M. und Kokkalis, A. und Mottura, L. und Serr, C. und Larrey, E. und Filippone, A. und Fischer, A. und Amato, M., "Helicopter Fuselage Drag Prediction: State of the art in Europe," in 39th AIAA Aerospace Sciences Meeting & Exhibit, Reno, 2001.

[6] A. D'Alascio, C. Castellin, B. Schöning, "Industrial validation of CFD solvers on medium and large helicopter fuselages," in European Rotorcraft Forum, Florenz, 2005.

[7] W. Khier, "Navier-Stokes Prediction of the Effect of the Skids on the Aerodynamics of Helicopter Fuselage in Forward Flight," in 35nd European Rotorcraft Forum, Maastricht, Holland, 2006.

[8] L. Rottmann, "Aerodynamic Analysis and Optimization of a Coaxial Helicopter Fuselage," in 22nd STAB/DGLR Symposium on New Results in Numerical and Experimental Fluid Mechanics XIII (151), Seiten 397-406. Springer International Publishing. STAB 2020 - 22. DGLR-Fachsymposium der STAB, Göttingen, 2020.

[9] Volpiani P., Chapelier J., Schwöppe A., Jägersküpper J., Champagneux S., "Simulating the Common Research Model using the new CFD software from ONERA, DLR and Airbus.," in AIAA 2023-3275, Gaylord National Harbor, 8 Jun 2023 https://doi.org/10.2514/6.2023-3275.

[10] Pedro Stefanin Volpiani, Jean-Baptiste Chapelier, Axel Schwöppe, Jens, "Aircraft Simulations Using the New CFD Software from ONERA, DLR, and Airbus," in Journal of Aircraft 61:3, 857-869, 2024.

[11] Langer S., Schwöppe A. and Leicht T., "Comparison and Unification of Finite-Volume Discretization Strategies for the Unstructured Node-Centered and Cell-Centered Grid Metric in TAU and CODA," in New Results in Numerical and Experimental Fluid Mechanics XIV, edited by Dillmann A., Heller G., Krämer E., Wagner C. and Weiss J., Springer Nature Switzerland, Cham, Switzerland, 2023.

[12] Thorsten Schwarz, Klausdieter Pahlke, "Generation of an Aadvanced helicopter Helicopter experimental Experimental aerodynamic Aerodynamic data Database for CFD validation Validation – The European GOAHEAD project," in Aerospace Science and Technology, Volume 19, Issue 1, 2012.

[13] Raddatz, J. und Fassbender, J.K, "Block Structured Navier-Stokes Solver FLOWer," in MEGAFLOW - Numerical Flow Simulation for Aircraft Design, 89, Seiten 27-44. Springer Verlag. Closing Presentation DLR Project MEGAFLOW, Braunschweig, 2005.

[14] D.Schwamborn, T.Gerhold, R.Heinrich, "The DLR Tau-code: Recent applications in research and industry," in European Conference on Computational Fluid Dynamics, Netherlands, 2006-04-09 - 2006-08-09.

[15] S. Allmaras, F. T. Johnson, and P. Spalart, "Modifications and clarifications for the implementation of the Spalart-Allmaras turbulence model," in Seventh International Conference on Computational Fluid Dynamics (ICCFD7), Big Island, Hawaii, 2012.

[16] A.F. Antoniadis, D. Drikakis, B. Zhong, G. Barakos, R. Steijl, M. Biava, L. Vigevano, A. Brocklehurst, O. Boelens, M. Dietz, M. Embacher, W. Khier, "Assessment of CFD methods against experimental Experimental flow Flow measurements Measurements for helicopter Helicopter flowsFlows," in Aerospace Science and Technology, Volume 19, Issue 1,Pages 86-100, 2012.

[17] Boelens, O.J., Barakos G., Biava M., Brocklehurst A., Costes, M., D'Alascio A., Dietz M., Drikakis D., Ekaterinaris, J., Humby I., Khier W., Knutzen B., Kok J., LeChuiton F., Pahlke K., Renaud T., Schwarz T., Steijl R., Sudre L., Zhong B., "The blind-test activity of the GOAHEAD project," in 33rd European Rotorcraft forumForum, Kazan, Russia, 2007.

[18] Khier W., Dietz M., Schwarz T., Wagner Ss, "Trimmed CFD Simulation of a Complete Helicopter Configuration," in 33rd European Rotorcraft Forum 2007, ERF33, For Journal of the American Helicopter Society Volume 1 to Volume 53, 2007.

[19] Steinbrenner, John P., "Construction of Prism and Hex Layers from Anisotropic Tetrahedra," in AIAA paper no. 2015-2296, 2015.